



Validation of circular dichroic spectroscopy of synthetic oligonucleotide PS2.M for K^+ concentration measurements

Luca Bruni¹, Massimo Manghi², Paola De Sanctis³, Cinzia Zucchini³, Simonetta Croci^{1,2,a} 

¹ National Institute for Biostructures and Biosystems, Rome, Italy

² Department of Medicine and Surgery, University of Parma, Parma, Italy

³ Department of Experimental, Diagnostic and Specialty Medicine (DIMES), Unit of Histology, Embryology and Applied Biology, Università di Bologna, Bologna, Italy

Received: 29 September 2021 / Accepted: 3 March 2022

© The Author(s) 2022, corrected publication 2022

Abstract The single-stranded synthetic oligonucleotide PS2.M is known to provide a basis for developing sensors since it tends to fold into structures called G-quadruplexes (G4) having characteristic topology and orientation with probabilities that depend on the chemical environment. The presence and concentration of cation species are among the key factors that determine the outcome of such a process. PS2.M and other aptamers have been used in several applications in conjunction with various probes, such as hemin, at the cost of increased technical complexity and applicability limitations. We instead validated the application limits of Circular Dichroic spectroscopy (CD) as only measurement method to assay PS2.M as K^+ sensor in a variety of solutions having different chemical complexity. The tested solutions range from simple NaCl and KCl solutions to chemically complex solutions like DMEM—Dulbecco's Modified Eagle Medium—which is widely used in a biological laboratory. PS2.M was also evaluated in solutions of $KHCO_3$ and D-ribose (K:D-rib), an antioxidant potassium compound, to compare its response to the simple KCl solution case. Our findings show that, within specific concentration applicability ranges, CD spectra can estimate the K^+ concentration in the examined water solutions even at high Na^+ concentrations with respect to K^+ and in the presence of antioxidant molecules.

1 Introduction

1.1 Ion potassium sensor and the G rich oligonucleotide sequences

Potassium ion sensors are intensively studied mainly due to the importance of the role potassium plays in fundamental biological processes, also in connection to pathological conditions [1–3]. Biosensors are of interest in K^+ measurements in biological solutions such as urine, blood or cell medium, *in vivo* measurements as well as to the assessment of extra- and intracellular K^+ concentration fluctuations, where a dynamic biosensor response is demanded. Along with conventional analytical techniques [4,5] two biosensor categories have stimulated the efforts of many researchers. The first exploits the properties of oligonucleotides sequences, with particular reference to the G-rich sequences [4,6–13] whereas the other uses potassium binding proteins (pbp) as active elements [14]. The second type of biosensors give excellent results by fusing pbps with cyan and yellow fluorescent protein variants to create K^+ sensors based on Förster resonance energy transfer—(FRET), but their development and production are considerable more complex and expensive compared to the first type. This paper attempts to determine and elucidate the limits and capabilities of CD spectra to indicate the actual K^+ concentration in a variety of solutions. It is known that the presence of cations such as K^+ and Na^+ and their concentration contributes to drive the PS2.M folding into the parallel and anti-parallel conformations but a survey of the actual quantitative response based on exclusively CD spectroscopy in a set of different solutions was, to our knowledge, still to be outlined.

1.2 G-quadruplex formation

When Watson and Crick published the model of DNA A and B in 1953, the predominant structure was interpreted to stand as a double stranded right-handed helix carrying the basis where the genetic code information is stored. Over and above that model some non-conventional secondary structures such as G-quadruplex (G4) were identified [15,16]. Gel formation of guanilyc acid at millimolar concentrations were known since the 19th Century but published by Bang only in 1910 and its structure was resolved 50 years later by Gellert and colleagues [17]. The crystal structure suddenly clarified the tetrameric association of guanines to form a G-quartet [17,18]. The coupling of the 4 guanines forms a G-quartet or tetrad, which is the planar square structural unit with the guanines located at the four vertices [19,20]. The base pairings are tied by Hoogsteen type H-bonds and each guanine

^a e-mail: simonetta.croci@unipr.it (corresponding author)

becomes a bond donor and an acceptor as well. In particular, the pairing of the N1 on the first guanine with the O6 on the second guanine along with the pairing of N2 on the first guanine with the N7 on the second guanine result in eight hydrogen bonds per G-tetrad [15]. The G4 structure is obtained only when at least two tetrads pile up on each other. The thermodynamic stability is provided by different players, such as hydrophobic interactions ($\pi - \pi$ interactions) among the tetrads, and monovalent or divalent cations [19,21]. It is crucial to point out that K^+ and Na^+ play an outstanding role in the G4 thermodynamic stability, as X-ray structural analysis proves that such ions fit into the G4 complex. In particular K^+ coordinates the eight guanine carbonyl oxygens (O6) protruding into the central hydrophobic cavity. Because of its atomic radius, Na^+ can coordinate only four oxygens. The role of the Na^+ and K^+ ions is to minimize the electrostatic repulsion forces among the carbonyl oxygens and to stabilize the G4 structure promoting its folding. Since K^+ has a higher coordination power with respect to Na^+ , it displays a larger affinity that leads to more structural stability. Weaker stabilizers, compared to K^+ and Na^+ , are Mg^{2+} , Li^+ and Cs^+ [15,22]. The G4 structure can be inspected by means of various techniques, such as X-ray crystallography, NMR, mass spectrometry, UV-VIS and circular dichroism (CD) spectroscopy. The last technique is a common approach to explore several aspects of the macromolecule secondary structures, G4s included. In particular, when the tetrads are piled up the DNA strand polarities contribute to determine the intensity and components of the CD spectra. CD allows the qualitative attributions of the spectra, defining three structural polymorphisms: parallel (positive peak at 264 nm, negative peak at 245 nm), antiparallel (positive peak at 295 nm, negative peak at 260 nm) and hybrid (positive peak at 295 nm, 260 nm, negative peak at 245 nm). Despite the fact that some exceptions to these features have been recognized, such as the interpretation of the shoulder 260 nm to 270 nm, the previous assignments are commonly accepted in case of G4 structures [23]. G-rich sequences are located in strategic regions of the genome and they play a central role such as gene expression regulation, structural and functional architecture of DNA and as important biological targets for cancer treatment [24]. Several G4 structures have been also studied as biosensors for detection of various analytes, such as metal ions in solutions having a wide range of complexity, organic molecules, nucleic acids, proteins and recently, pathogens including SARS-CoV-2 [8,25].

1.3 Technical aspects of G4-based biosensors application

G4 biosensors are often coupled to probes such as hemin, an anionic porphyrin known as a cofactor of proteins and enzymes like peroxidases. Once G4 has shaped up hemin binds to G4 to form a DNAzyme. In order to use DNAzyme for measuring the K^+ concentration one should also monitor the catalytic activity through an appropriate reaction mediated by substrates such as ABTS (2,2-azino-bis(3-ethylbenzthiazoline-6-sulphonic acid)) or luminol and H_2O_2 . These molecules are oxidized (ABTS or luminol) and reduced (H_2O_2) and the reaction is monitored by UV-VIS or chemiluminescence spectroscopy. The requested role of K^+ in the peroxidase activity is to induce the folding of secondary and tertiary structures of guanine-rich oligonucleotide sequences, such as an apoenzyme, capable to bind hemin and to perform like a peroxidase [6,9,26], but the stability and kinetics of PS2.M folding are affected by the binding of hemin (data not shown), which is a necessary component of the whole process. Since DNAzyme catalyzes the ABTS or Luminol oxidation by H_2O_2 the presence of antioxidant molecules in the tested solutions interfere with DNAzyme activity reducing H_2O_2 thus biasing the value of the K^+ concentration [9]. Thus the CD spectroscopy validation of PS2.M in a probeless experimental setup enables the adoption of such oligonucleotide as biosensor in chemical conditions where otherwise hemin would interfere with the PS2.M conformation stability. The absence of hemin permits to measure K^+ in the presence of oxidant or antioxidants that would disrupt the DNAzyme activity and avoids the adoption of substrates [27]. Other interesting potassium biosensors are based on G4-crystal violet complexes [13] where CV fluorescence variations are tied to the potassium concentration. These sensors are coupled to the CV molecule and also in this case interactions with oxidizing or reducing molecules cannot be ruled out thus increasing the system complexity.

1.4 CD spectroscopy-based validation of the K^+ biosensor

In order to have a preliminary evaluation of the PS2.M folding induced by the presence of K^+ , CD spectra of K^+ solutions at concentrations ranging between 0 mM and 10 mM and constant Na^+ concentration of 80 mM were collected. Likewise spectra were collected also for solutions of DMEM and K^+ at the same concentrations. We then took spectra of solutions of KCl and K:D-rib (a water solution of D-ribose and $KHCO_3$) separately for equivalent K^+ concentrations with the purpose of comparing the response observed in the CD spectra and rule out the possibility that K:D-rib could interfere with the PS2.M K^+ driven folding process. The adoption of a probeless sensor is crucial when measuring K^+ released by dissociation of substances such as K:D-rib which have antioxidant properties because they interact with the DNAzyme and its substrates (H_2O_2 and ABTS) thus demanding the interaction between them to be taken into account and thus adding complexity to the experimental data interpretation. In the last experiment PS2.M was tested in DMEM with K:D-rib. In this experiment the crucial point of the contribution to the overall K^+ concentration brought by DMEM and K:D-rib together with the solution complexity were taken into account.

2 Materials and methods

2.1 The oligonucleotide

The PS2.M (5'-GTGGGTAGGGCGGGTTGG-3') single-stranded oligonucleotide was purchased from Tema Ricerca srl, Bologna, Italy. The lyophilized oligonucleotide was promptly reconstituted by adding TE buffer: Tris (10 mM) (Sigma-Aldrich) 7.5 pH and EDTA (0.1 mM) (Sigma-Aldrich) in order to obtain a stock concentration (100 μ M) and then stored at -20°C . The DNA was quantified by UV/VIS spectroscopy at RT; the molar extinction coefficient is $\epsilon_{254} = 191\,085.2\text{ M}^{-1}\text{ cm}^{-1}$. Before quantification, the DNA solution was heated at 95°C for 5 min then cooled back at 0°C (water and ice) for 10 min.

2.2 Folding solutions

Each folding solution was prepared from a starting solution composed of PS2.M (10 μ M) and EDTA (0.1 mM) then adding the solutions described in the following sections. The wanted Na^{+} and K^{+} concentrations were obtained adding distilled water so as to reach the final volume of 400 μ l. The DNA and the EDTA concentrations were in agreement with the protocol outlined by Paramasivan et al. [28]. The folding reactions occurred at room temperature (RT), in the darkness and they took 24h to complete.

2.3 Solutions with NaCl and KCl

The simplest PS2.M folding process promoted by K^{+} in the presence of Na^{+} at 80 mM was measured in a series of 5 samples where the K^{+} concentrations were 0, 2.5, 5, 7.5 and 10 mM. The Na^{+} source was NaCl (Sigma-Aldrich) while those of K^{+} was KCl (Sigma-Aldrich). These samples were obtained in agreement with Sect. 2.2.

2.4 Solutions with DMEM and KCl

Dulbecco's Modified Eagle Medium (DMEM low glucose—Gibco) was the most complex solution tested. DMEM is a widely known cancer cell medium. When DMEM is supplemented with fetal bovine serum (FBS—Gibco), L-glutamine (L-Glut—Gibco) penicillin/streptomycin (pen/strep Gibco) is called “complete DMEM”. In this paper, unless explicitly declared, with DMEM we mean the complete form of the medium whose chemical and biological composition is a key factor to be taken into account. To mimic a human cell line culturing process, DMEM was supplemented with FBS (10%), L-Glut (1%) and pen/strep (1%). Since FBS itself is a source of Na^{+} and K^{+} after the preparation their concentration in DMEM was 170.8 mM and 6.45 mM, respectively. Measurements were carried out on samples of DMEM and KCl at 0, 5, 7.5, 11.2, 15 mM. Due to the FBS contribution the solutions had actual K^{+} concentrations of 6.45, 11.45, 13.95, 17.65 and 21.45 mM. For experimental reasons DMEM supplemented with KCl were diluted 1:2 with respect to final volume (400 μ l) that was obtained adding distilled water (see Sect. 2.2). Thus in the measured solutions the Na^{+} final concentration was 85.4 mM and the K^{+} final concentrations were 3.23, 5.73, 6.98, 8.83, 10.73 mM.

2.5 Comparison between K:D-rib and KCl

With the purpose of estimating the possible interference on the process brought about by the antioxidant action of K:D-rib (see Sect. 1.1) a folding solution of K:D-rib, which in its own right is a contributor of K^{+} , was measured to verify whether the PS2.M folding could be explained in terms of the overall K^{+} only. A K:D-rib (250 mM) stock solution was prepared weighting of D-ribose (Sigma-Aldrich) (150 mg) and of KHCO_3 (Prolabo) (300 mg) in distilled water (4 ml), corresponding to a molar ratio of 1:3 and gently mixing the solution waiting for the CO_2 dissipation [29]. To assay K:D-rib sample, the folding solution was prepared by adding K:D-rib stock solution and distilled water to the starting solution (see Sect. 2.2) to obtain K:D-rib at 5 mM. PS2.M folding in the presence of K:D-rib 5mM was compared with those in the presence of a sample carrying KCl 15 mM, in agreement with what has been detailed in the Sect. 2.2 [10]. 15 mM it is also the highest KCl concentration used in the experiment with DMEM.

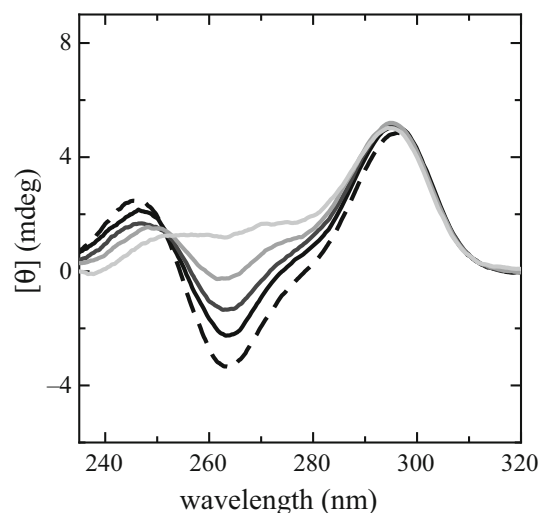
2.6 Solutions with DMEM and K:D-rib

Lastly the CD spectra were measured for a batch of DMEM solutions supplemented with K:D-rib at 0, 1.5, 2.5, 3.5, 4.0, 5.0, 6.0, 7.0, 10 and 12 mM. For experimental reasons such samples were diluted 1:2 with respect to final volume (400 μ l) that was obtained by adding distilled water (see Sect. 2.2). Considering the K:D-rib stoichiometry (Sect. 2.5) and the dilutions the Na^{+} concentration was 85.4 mM and the final sample K^{+} concentrations were: 3.22, 5.47, 6.97, 8.47, 9.23, 10.73, 12.23, 13.73, 18.23 and 21.23 mM.

2.7 Circular dichroism

The CD spectra were collected by means of a J-715 spectropolarimeter (Jasco), endowed with an electronic Peltier to control the temperature of the cell holder. Spectra were measured in the 235 nm to 320 nm wavelength range at a scanning speed of 50 min^{-1} , data pitch of 0.2 nm, bandwidth of 1 nm and time response of 8 s. Samples were held in a quartz cell with an optical path

Fig. 1 CD spectra of PS2.M (10 μ M) folded in the presence of the starting solution (distilled water and EDTA) supplemented with NaCl (80 μ M) and KCl at the concentrations of 0 μ M (dashed black spectrum), 2.5 mM (black solid spectrum), 5 mM (dark gray solid spectrum), 7.5 mM (gray solid spectrum) and 10 mM KCl (light gray spectrum). The experimental data were taken from our previous published paper [10]



of 2 mm. The lamp holding chamber was flushed with a constant nitrogen stream to prevent ozone formation. All spectra were acquired at 20 °C and the final spectra were computed by averaging three subsequent spectra acquisitions. A reference spectrum was measured by acquiring a spectrum of a sample with TE instead of DNA and then subtracted from each sample spectrum.

3 Results and discussion

3.1 Solutions with NaCl and KCl

We already described in [10] the PS2.M capability as K^+ biosensor in solutions of NaCl and KCl. Examples of the spectra obtained in such experiment are shown in Fig. 1. These spectra have the typical spectral form characterizing antiparallel G4 structures as demonstrated also in [21,28]. Such spectra display two positive peaks at 295 nm and 245 nm, respectively, and a negative one at 265 nm. Spectra amplitudes at 245 nm and 265 nm vary with the KCl concentration. In particular, the component at 245 nm decreases and slightly shifts towards longer wavelengths while the component at 263 nm becomes less pronounced, almost vanishing at 10 mM of KCl. The third component at 295 nm is nearly constant in intensity at all KCl concentrations, beside a shift towards shorter wavelengths and a fourth positive shoulder at 275 nm. The component at 275 nm shows up when K^+ is present in the solution getting more pronounced as the KCl concentration grows. The largest ellipticity differences are observed at 263.6 nm. The ellipticity at 263.6 nm in such spectra, plotted as a function of $[K^+]$ (Fig. 2), exhibits a linear dependence, whose linear fit is assumed to be the biosensor calibration curve. Figure 2 experimental data were taken from our previous published paper [10] (Fig. 12, top panel, blue diamonds). In the reported potassium range the biosensor has a sensitivity of 0.44 ± 0.02 mdeg/mM [10].

3.2 Solutions with DMEM and KCl

Spectra of folded PS2.M in solutions of KCl and DMEM are shown in Fig. 3. The components at 265 nm and 295 nm show the same kind of modifications of the NaCl–KCl experiment, suggesting that PS2.M still folds into a G4 structure, despite the complexity of DMEM. The ellipticity signal magnitude at 295 nm weakly depends on the K^+ concentration and exhibits a small reduction corresponding to the growth of the component at 265 nm. The wavelength where the CD spectra exhibit the largest variation is 264.6 nm. The wavelength ellipticity plotted as a function of K^+ has been adopted to characterize the biosensor response (Fig. 4) defining a resolution and a sensitivity of 0.8 mM and 1.10 ± 0.03 mdeg/mM, respectively.

3.3 Comparison between K:D-rib and KCl

As explained in Sect. 2.5 we carried out these measures with the aim of understanding whether the presence of an antioxidant molecule (K:D-rib) somehow interferes with the folding of PS2.M, whether this substance could be considered a net contributor of K^+ to the solution and to what extent the spectra could be interpreted by the K^+ concentration. For this purpose two spectra were measured: the first of a PS2.M solution in the presence of K:D-rib at 5 mM, which means a K^+ concentrations of 15 mM, and the second in the presence of KCl at 15 mM. The two corresponding spectra are shown together in Fig. 5. Both of them show the same intensity absorption at 295 nm (the highest peak), 250 nm (the lowest positive peak) and 272 nm (the positive shoulder), the component at 295 nm being characteristic of an antiparallel structure [26]. The positive shoulder at 272 nm becomes noticeable according to the spectra of the NaCl–KCl experiment. In these experiments where both KCl and K:D-rib [29,30] were involved, CD

Fig. 2 CD ellipticity values at 263.6 nm as a function of the different K^+ concentrations in the presence of 80 mM NaCl. The black solid line is the fitted linear regression. The experimental data were taken from our previous published paper [10]

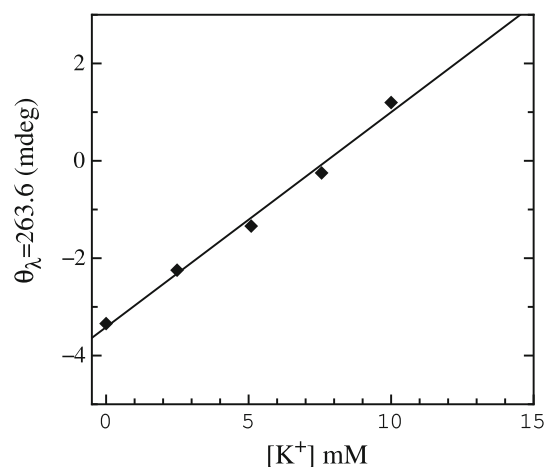


Fig. 3 CD spectra of PS2.M (10 μ M) folded in the presence of the starting solution (distilled water and EDTA) supplemented with DMEM (turquoise spectrum) [Na⁺] = 85.4 mM and [K⁺] = 3.23 mM; DMEM treated with KCl 5 mM (light blue spectrum) [Na⁺] = 85.4 mM and [K⁺] = 5.73 mM; DMEM treated with KCl 7.5 mM (blue spectrum) [Na⁺] = 85.4 mM and [K⁺] = 6.98 mM; DMEM treated with KCl 11.2 mM (dark purple spectrum) [Na⁺] = 85.4 mM and [K⁺] = 8.83 mM; DMEM 15 mM KCl (black spectrum) [Na⁺] = 85.4 mM and [K⁺] = 10.73 mM

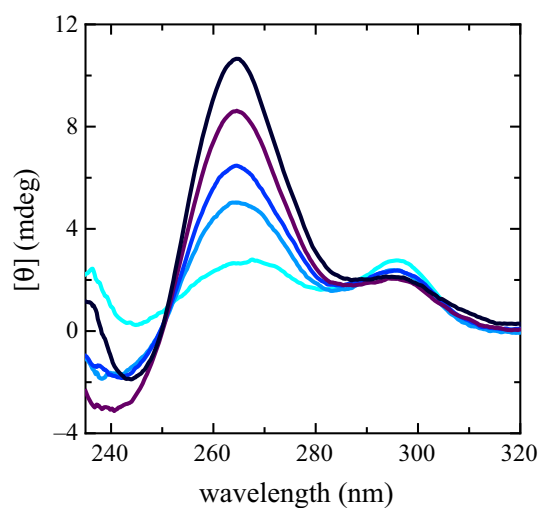
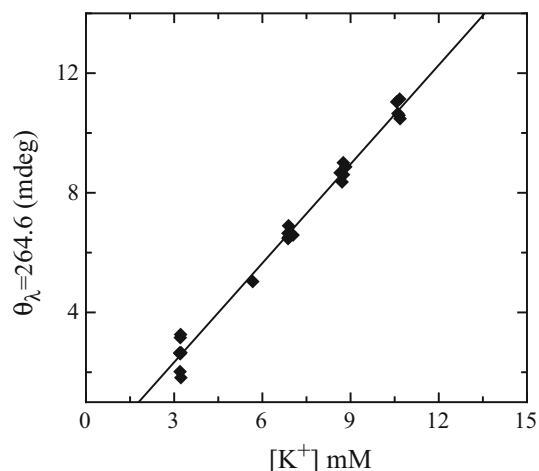


Fig. 4 CD ellipticity values at 264.6 nm as a function of the different K^+ concentrations coming from several PS2.M independent folding experiments in the presence of DMEM and DMEM treated with increasing KCl concentrations. The black solid line is the fitted linear regression. For one run, the CD spectra corresponding to the whole K^+ concentrations investigated, are plotted in Fig. 3



spectra demonstrate the two K^+ sources induce PS2.M to fold according to the same G4 structure, despite the different chemical identities of K:D-rib and KCl; a similar behaviour was seen in other oligonucleotide sequences by Rehm and Colleagues [31] where identical spectra were also induced by different potassium salts, therefore not dependent on the anion.

Fig. 5 CD spectra of PS2.M (10 μ M) folded in the presence of the starting solution (distilled water and EDTA) supplemented with 5 mM of K:D-rib (solid spectrum) and KCl 15 mM (red dashed spectrum)

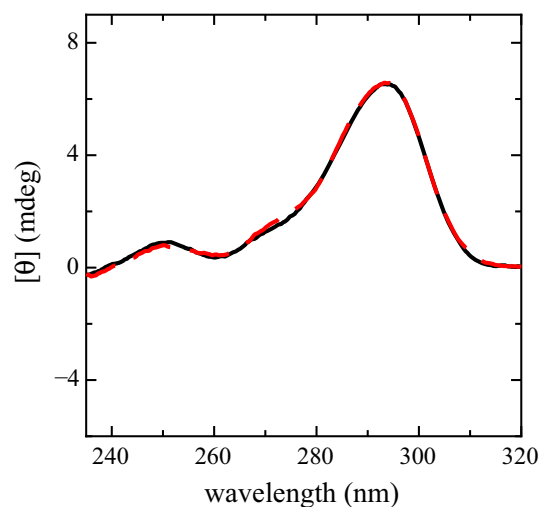
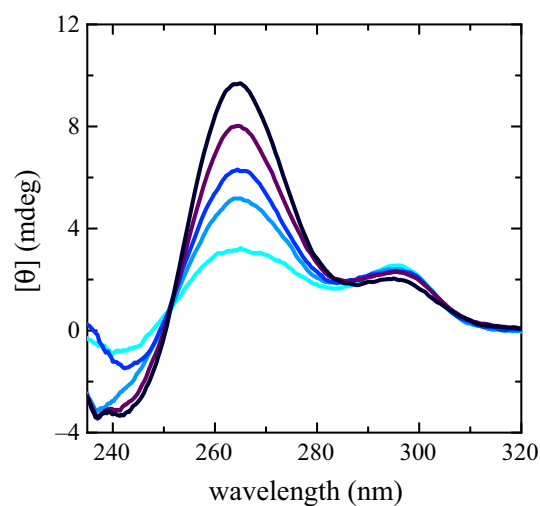


Fig. 6 CD spectra of PS2.M (10 μ M) folded in the presence of the starting solution (distilled water and EDTA) supplemented with: DMEM (turquoise spectrum) [Na⁺] = 85.4 mM and [K⁺] = 3.22 mM; DMEM treated with K:D-rib 1.5 mM (light blue spectrum) [Na⁺] = 85.4 mM and [K⁺] = 5.47 mM; DMEM treated with K:D-rib 2.5 mM (blue spectrum) [Na⁺] = 85.4 mM and [K⁺] = 6.97 mM; DMEM treated with K:D-rib 3.5 mM (dark purple spectrum) [Na⁺] = 85.4 mM and [K⁺] = 8.47 mM; DMEM treated with K:D-rib 5.0 mM (black spectrum) [Na⁺] = 85.4 mM and [K⁺] = 10.73 mM



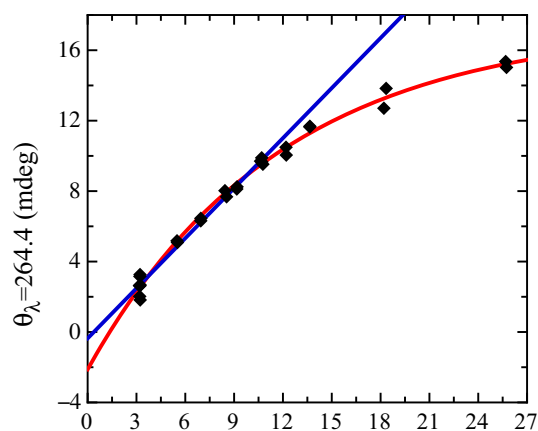
3.4 Solutions with DMEM and K:D-Rib

Finally, spectra generated by solutions of PS2.M folding in the presence of DMEM treated with increasing concentrations of K:D-rib (0 mM to 12 mM) were measured. These samples followed the same experimental procedure of the previous set, with K:D-rib playing the role of KCl. Also in this experiment the wavelength at which the CD spectra show the largest variations were observed at about 264.4 nm as shown in Fig. 6, where a few selected spectra are displayed with the purpose of exemplify their behaviour. In this case too PS2.M folds according to a G4 structure. Even for this batch of samples, the CD spectra display the same two positive components at 265 nm and 295 nm with the component at 295 nm only weakly depending on the K:D-rib concentration. The presence of isodichroic points at 250 nm and 285 nm could be a sign of a two state transition from the antiparallel to parallel conformation similarly to what Zhang et al. observed in [12] for the PW17 oligonucleotide. No evident shift is present at 265 nm which displays a marked dependence on the K:D-rib concentration. Similarly to the other experiments, the absorption value at 264.6 nm plotted as a function of the overall K⁺ concentration is used to describe the response of the sensor, being the K⁺ concentrations determined by contributions from both DMEM and K:D-rib. A calibration curve in the studied range can be obtained with an exponential fit, as shown in Fig. 7. The absorption spectrum changes over the whole K:D-rib concentration range but the linear response is best obtained for [K⁺] < 11 mM, leading to a resolution of 1 mM and sensitivity of 0.95 ± 0.03 mdeg/mM. All the spectra data and the datasets analysed during the current study are available as supplementary information to this paper.

4 Conclusions

Even in a probeless experimental setup PS2.M reveals K⁺ biosensor capabilities in water solutions in the presence of an excess of Na⁺. The sensitivity tests began with the simplest water solution composed by 80 mM of NaCl and an increase KCl concentration.

Fig. 7 CD absorption values at 264.4 nm as a function of the overall K^+ concentrations coming from DMEM and DMEM treated with K:D-rib. The plotted values are collected by several independent experiments of PS2.M folding. The lilac line is the fitted linear regression as if the biosensor would not have been saturated. The red one is the fitted exponential curve. They share the linear trend for $[K^+] < 11$ mM. CD spectra corresponding to the some of the K^+ concentrations investigated are plotted in Fig. 6



Resolution and sensitivity confirm the reliability of PS2.M as a K^+ biosensor in such conditions. The spectra suggest that K:D-rib works as a K^+ source through dissociation, since we observed the same spectra we had when the folding was promoted by adding KCl, which we take as a confirmation that PS2.M folds according to a G4 structure precisely in the same way. In addition, according to CD spectra D-ribose seems not to affect neither the PS2.M folding nor the K^+ availability. Next we tested the biosensor performance into a water solution with significant complexity such as DMEM treated with KCl and K:D-rib. In both cases PS2.M displayed a linear response with respect to the K^+ concentration confirming the performance expectations, even at significantly higher Na^+ concentrations.

This is certainly a very promising result. In fact other sequences studied to date such as PW17 [12] lose the linear response when in the presence of a high concentration of sodium like in extracellular matrices. The sensors presented in this paper and in [13] work in a similar way, attaining their linear behavior at similar potassium ranges and modulating the sodium concentration in order to obtain the optimal value in which the sensors work. Still in the conditions outlined the PS2.M sensor is based only on the G4 complex, while maintaining a linear response. Moreover it shows a much higher slope (1.10 ± 0.03 mdeg/mM) in the complex solution with respect to the NaCl–KCl buffer solutions (0.44 ± 0.02 mdeg/mM), hence a higher sensitivity. This is not the case of the Crystal violet–G-quadruplex complexes tested on urine where the slope of the linear plot was not so large as that in the synthetic matrix [13]. It is important to emphasize how the strength of this sensor is precisely its ability to work at concentrations of Na^+ useful for biological matrices and in the absence of other fluorescent probes.

The resolution is about the same (1 mM) in all the three calibration curves presented. The sensitivity are higher in the presence of DMEM treated with K:D-rib and KCl, with respect to the simplest solution, suggesting that the G4 dynamic, switching from antiparallel or mixed type conformations to parallel ones at defined potassium concentrations, depends on the solution compositions and complexity. This suggests that different calibration curves be made for each investigated solution in order to have the biosensor response correct readings. A similar experiment was performed using two non-synthetic oligonucleotides Pu27 and Pu23 (a Pu27 mutant) [11]. PS2.M displays a higher sensitivity and resolution respect to Pu27 and Pu23, that may be connected to their thermodynamic instability. Pu27 and Pu23 have relevant roles into the gene expression regulations, so it is not conceivable to have an unstable gene expression regulator. PS2.M could also work as a K^+ biosensor in biological matrices, such as cell supernatants, groundwater, marine or lacustrine water.

Supplementary Information The online version contains supplementary material available at <https://doi.org/10.1140/epjp/s13360-022-02581-2>.

Acknowledgements This material is based upon project supported by Museo Storico della Fisica and Centro Studi e Ricerche Enrico Fermi (P0034).

Funding Open access funding provided by Università degli Studi di Parma within the CRUI-CARE Agreement.

Open Access This article is licensed under a Creative Commons Attribution 4.0 International License, which permits use, sharing, adaptation, distribution and reproduction in any medium or format, as long as you give appropriate credit to the original author(s) and the source, provide a link to the Creative Commons licence, and indicate if changes were made. The images or other third party material in this article are included in the article's Creative Commons licence, unless indicated otherwise in a credit line to the material. If material is not included in the article's Creative Commons licence and your intended use is not permitted by statutory regulation or exceeds the permitted use, you will need to obtain permission directly from the copyright holder. To view a copy of this licence, visit <http://creativecommons.org/licenses/by/4.0/>.

References

1. C.C. Luca, G. Nadayil, C. Dong, F.B. Nahab, E. Field-Fote, C. Singer, *J. Neurol. Sci.* **379**, 7, ISSN 0022-510X (2017)
2. R. Maglemose, A. Hedegaard, J. Lehnhoff, K.P. Dimintyanova, M. Moldovan, L. Grøndahl, C.F. Meehan, *Exp. Neurol.* **292**, 154, ISSN 0014-4886 (2017)

3. R. Eil, S.K. Vodnala, D. Clever, C.A. Klebanoff, M. Sukumar, J.H. Pan, D.C. Palmer, A. Gros, T.N. Yamamoto, S.J. Patel et al., *Nature* **537**(7621), 539, ISSN 0028-0836 (2016)
4. Q.J. Wan, P. Kubáň, J. Tanyanyiwa, A. Rainelli, P.C. Hauser, *Anal. Chim. Acta* **525**(1), 11 (2004)
5. V. Chromy, J. Fischer, *Clin. Chem.* **23**(4), 754, ISSN 0009-9147 (1977)
6. X. Yang, T. Li, B. Li, E. Wang, *Analyst* **135**(1), 71 (2010)
7. H. Yaku, T. Murashima, D. Miyoshi, N. Sugimoto, *Molecules* **17**(9), 10586, ISSN 1420-3049 (2012)
8. B. Ruttkay-Nedecký, J. Kudr, L. Nejd, D. Maskova, R. Kizek, V. Adam, *Molecules* **18**(12), 14760, ISSN 1420-3049 (2013)
9. J. Kosman, B. Juskowiak, *Anal. Chim. Acta* **707**(1–2), 7 (2011)
10. L. Bruni, M. Manghi, S. Croci, *Eur. Phys. J. Plus* **133**(8), 337 (2018)
11. L. Bruni, *Il nuovo cemento C* **42**(5), 1 (2019)
12. D. Zhang, J. Han, Y. Li, L. Fan, X. Li, *J. Phys. Chem. B* **120**(27), 6606 (2016)
13. D.M. Kong, J.H. Guo, W. Yang, Y.E. Ma, H.X. Shen, *Biosens. Bioelect.* **25**(1), 88 (2009)
14. H. Bischof, S. Burgstaller, M. Waldeck-Weiermair, T. Rauter, M. Schinagl, J. Ramadani-Muja, W.F. Graier, R. Malli, *Cells* **8**(5), 492 (2019)
15. D. Bhattacharyya, G. Mirihana Arachchilage, S. Basu, *Front. Chem.* **4**, 38 (2016)
16. D. Yang, K. Okamoto, *Fut. Med. Chem.* **2**(4), 619 (2010)
17. M. Gellert, M.N. Lipsett, D.R. Davies, *Proc. Natl. Acad. Sci. USA* **48**(12), 2013 (1962)
18. X.B. Zhang, R.M. Kong, Y. Lu, *Ann. Rev. Anal. Chem. (Palo Alto, Calif.)* **4**(1), 105 (2011)
19. G.N. Parkinson, M.P.H. Lee, S. Neidle, *Nature* **417**(6891), 876 (2002)
20. Y. Chen, D. Yang, *Curr. Protocols Nucl. Acid Chem.* **50**(1), 15 (2012)
21. N. Maizels, L.T. Gray, *PLoS Genet.* **9**(4), e1003468 (2013)
22. S. Burge, G.N. Parkinson, P. Hazel, A.K. Todd, S. Neidle, *Nucl. Acids Res.* **34**(19), 5402 (2006)
23. R. del Villar-Guerra, J.O. Trent, J.B. Chaires, *Angew. Chem. Int. Edn.* **57**(24), 7171, ISSN 1433-7851 (2018)
24. R. Hänsel-Hertsch, M. Di Antonio, S. Balasubramanian, *Nat. Rev. Mol. Cell Biol.* **18**, 279 (2017)
25. H. Xi, M. Juhas, Y. Zhang, *Biosens. Bioelect.* **167**, 112494, ISSN 0956-5663 (2020)
26. P. Travascio, Y. Li, D. Sen, *Chem. Biol.* **5**(9), 505 (1998)
27. D. Huang, B. Ou, R.L. Prior, *J. Agric. Food Chem.* **53**(6), 1841, ISSN 0021-8561 (2005)
28. S. Paramasivan, I. Rujan, P.H. Bolton, *Methods* **43**(4), 324 (2007)
29. L. Bruni, A.A. Babarinde, I. Ortalli, S. Croci, *Cancer Cell Int.* **14**(77) (2014)
30. S. Croci, L. Bruni, S. Bussolati, M. Castaldo, M. Dondi, *Cancer Cell Int.* **11**, ISSN 1475-2867 (2011)
31. C. Rehm, I.T. Holder, A. Groß, F. Wojciechowski, M. Urban, M. Sinn, M. Drescher, J.S. Hartig, *Chem. Sci.* **5**(7), 2809 (2014)